Assessing the Impact of Groundwater Saturation Excess Runoff on Hydrologic Features and Processes in a Watershed Modeling Setting

Salam A. Abbas[1*], Ryan T. Bailey[1], Jeffrey G. Arnold[2], and Michael J. White[2]

[1]Department of Civil and Environmental Engineering, Colorado State University, USA.

[2]Grassland Soil and Water Research Laboratory, USDA–ARS, Temple, TX, 76502, USA.

Corresponding author: Salam A. Abbas (salam.a.abbas@colostate.edu)

Key Points:

- We evaluate the effect of groundwater saturation excess flow on hydrologic features (wetlands) and temporal patterns of watershed water yield.
- We demonstrate relationships between precipitation, recharge, saturation excess flow, and streamflow before and during storm events.
- We compare locations of consistent groundwater saturation excess flow (simulated) with mapped wetlands.

Abstract

Groundwater saturation excess flow can be a major surface runoff mechanism in humid regions, characterized by shallow aquifers and soil profiles that become saturated during wet periods or intense storm events. This process often plays an important role in the creation and maintenance of groundwater-dependent ecosystems and the overall water yield of a watershed. In this paper, we examine the process of groundwater saturation excess flow and assess its influence on hydrologic features (wetlands) and temporal patterns of watershed water yield. We do this by applying a surface-subsurface hydrologic model (SWAT+ with the physically based spatially distributed *gwflow* module for groundwater storage and flow) to the Little River Watershed, Georgia, USA, which has a high baseflow fraction and contains numerous wetlands, and for which groundwater saturation excess flow has been noted in past studies. The model is calibrated and tested against measured streamflow and groundwater head for the period 2000-2015, with and without groundwater saturation excess flow included in the *gwflow* module. Model results indicate that including groundwater saturation excess flow improves hydrologic estimation, and demonstrate connections between precipitation, recharge, saturation excess flow, and streamflow before and during storm events. Finally, we compare locations of consistent groundwater saturation excess flow (simulated) with mapped wetlands, demonstrating that the model can be used to explore impacts of system changes (land use, climate, management) on wetland development and maintenance.

Plain Language Summary

In humid regions with high rainfall rates, groundwater can rise to the surface and discharge to the land surface and nearby wetlands and streams. This process is valuable for sustaining ecosystems that depend on groundwater and for general streamflow generation. In this study, we examine how this process of groundwater saturation excess flow influences hydrology and wetland development in the Little River Watershed in Georgia, USA. We employ a computer model to investigate this process and how it effects surface runoff, streamflow rates, and the presence of wetlands. The model is tested by comparing output to measured streamflow and groundwater levels during the 2000-2015 period. The results reveal that including groundwater saturation excess flow in the model helps us better understand water movement in the watershed, particularly during and after rain storms. We also look at how this groundwater process connects with water recharge, streamflow, and rainfall. Finally, we compare areas of consistent groundwater saturation excess flow to areas of mapped wetlands. This work enables us to understand how groundwater saturation excess flow effects the environment, and provides a modeling tool for studying relationships between climate, management, and groundwater-dependent ecosystems.

1 Introduction

Accurate prediction of hydrologic processes is essential for effective watershed management, given the complexity of watershed systems influenced by various factors including land use, climate, and anthropogenic impacts (e.g., Abbas and Xuan, 2019; Du et al., 2022; Gyamfi et al., 2016). Hydrologic models assist water resource managers in comprehending the impacts of natural and anthropogenic factors on, for example, hydrological features, optimizing reservoir operations, and predicting changes in water resources (Wu and Xu, 2007; Mengistu et al., 2021). Proper representation of hydrologic processes, including surface runoff, groundwater recharge, and groundwater seepage, is vital for simulating streamflow and groundwater head in a distributed hydrologic model in an accurate fashion. Of these processes, groundwater seepage is often neglected when applying watershed models.

Groundwater seepage at the land surface, often referred to as "groundwater discharge" or "groundwater saturation excess runoff", occurs when the water table intersects local topography (Bear, 1972; Deitchman and Loheide, 2009; Rath et al., 2023). This seepage water can play an important role in 1) the generation and maintenance of groundwater-dependent ecosystems (GDEs) such as wetlands and fens (i.e., wetlands reliant on groundwater discharge) (Shedlock et al., 1993; Hunt et al., 1996; Winter, 1999; Batelaan et al., 2003; Dekker et al., 2005; Feinstein et al., 2019; Lamber et al., 2022); and 2) the generation of surface water flow and overall water yield of a watershed, particularly during storm events that cause high groundwater levels (Beven, 1989; Ruprecht and Schofield, 1989; Bari et al., 1996; Kazmierczak et al., 2016). For wetlands and fens, groundwater provides essential supplies of water, nutrients, and heat (Kløve et al., 2011). These internal (GDEs) and response (streamflow generation) features of a watershed system often are threatened by land use activities, climate change, and groundwater extraction (Dekker et al., 2005; Brown et al., 2010; Kløve et al., 2011; Aldous and Bach, 2014).

Providing informed water management in watersheds wherein groundwater seepage plays a significant role in either GDE development or streamflow generation requires the establishment of dynamics relationships between watershed features, weather patterns, groundwater storage and flow, wetland locations, and streams (Batelaan et al., 2003; Brown et al., 2010; Kløve et al., 2011). These relationships, however, have not yet been defined on the watershed scale. Many studies have investigated and quantified the generation of groundwater seepage along hillslopes (e.g., Cloke et al., 2003; Beaugendre et al., 2006; Scudeler et al., 2017; Bizhanimanzar et al., 2019; Rath et al., 2023), although at small spatial scales and under controlled numerical experiments. In connection with GDEs, Sampath et al. (2016) and Feinstein et al. (2019) used physically based groundwater models (MODFLOW) to simulate interactions between groundwater and fens. However, they used steady-state conditions and neglected other land surface features (e.g., evapotranspiration). For streamflow generation, semi-distributed models such as SWAT (Easton et al., 2008; White et al., 2011; Hoang et al., 2017; Steenhuis et la., 2019) have implemented saturation excess routines, but only in terms of soil water storage and not in relation to groundwater storage or a rising water table within a physically based framework. Other modeling studies in low-gradient watersheds (Bosch et al., 2010; Rathjens et al., 2015) have noted that correct simulation of daily or monthly streamflow requires the inclusion of interactions between groundwater and the soil surface.

In general, there is a lack of information on large-scale spatial and temporal relationships between groundwater saturation excess flow, GDEs, and streamflow generation, that include the influence of watershed inputs (weather, land use) and hydrologic processes. These relationships and influences should be quantified in a coupled surface-subsurface manner to inform planning and protection strategies for wetlands, fens, and general water supply. Also, to our knowledge, no studies have quantified the effect of groundwater saturation excess runoff on hydrological processes in a large-scale watershed system.

The objective of this paper is to quantify the impact of groundwater saturation excess flow on hydrologic features and hydrologic processes in a humid, regional watershed.

Specifically, we aim to quantify the impact of groundwater saturation excess flow on hydrologic fluxes, streamflow generation, and wetland development and location. For the latter, we employ a method similar to Feinstein et al. (2019), in which they compared locations and rates of model-simulated groundwater seepage to known locations of fens. In addition, we relate the frequency of groundwater saturation excess flow (i.e., the fraction of time that excess flow occurs) to known wetland locations.

To achieve these objectives, we apply the SWAT+ hydrologic model, amended with the *gwflow* module (Bailey et al., 2020), to the Little River Watershed (2,309 km^2), Upper Suwannee River Basin, south-central Georgia, USA. This watershed has been studied extensively as an experimental watershed (Bosch et al., 2007), with results suggesting significant contribution of groundwater saturation excess runoff to streamflow (Bosch et al., 1996; Inamdar et al., 1999; Bosch et al., 2017). The *gwflow* module simulates groundwater storage and head in a process-based manner using a collection of grid cells connected to SWAT+ hydrologic response units and channels, providing a powerful tool for simulating water movement in a surface-subsurface system. The combined model is run on a daily time step from 2000 to 2015, and tested against streamflow at multiple gaging sites, groundwater head at multiple monitoring wells, and the location of established wetlands. The model is run with and without the groundwater saturation excess flow mechanism active in the modeling code, to determine its effect on watershed hydrology.

In addition to hydrologic insights gained from applying the modeling method, the model can, in general, be used as a tool to explore the impact of system changes (climate, land use, management) on wetland development, wetland maintenance, water supply, and conjunctive supply of surface water and groundwater. We note that the basic SWAT+*gwflow* model set-up for the Little River Watershed has previously been outlined in Bailey et al. (2023), in which the SWAT+*gwflow* set-up was demonstrated for several watersheds across the United States. This work builds on previous application by adding model calibration and testing, and a detailed exploration of the effect of saturation excess flow on watershed hydrology.

2 Materials and Methods

2.1 Study Area

We apply modeling methods to the Little River Watershed (2,309 km^2), Upper Suwannee River Basin, south-central Georgia. Figure 1 shows a map of elevation, locations of USGS river gage stations used for model testing, locations of USGS monitoring wells used for testing, locations of weather stations, water bodies, and wetland delineation. Wetland locations are provided by the National Wetlands Inventory of the U.S. Fish and Wildlife Service (accessed October 2023). This watershed was selected due to reported hydraulic connection between streams and the shallow aquifer and the presence of groundwater saturation excess flow (Bosch et al., 2017).

The study area has a humid subtropical climate, with mild winters and hot humid summers. In the summer months, there is typically a significant increase of streamflow due to high-intensity thunderstorms. The average yearly precipitation is 1,287 mm, while the mean temperature for the year is 19 °C. Evapotranspiration accounts for approximately 70% of annual precipitation (Sheridan, 1997). Elevations in the watershed range from 34 to 148 meters (Figure 1A).

Land use (Figure 2A) comprises forest (45%), mostly evergreens and hardwoods in riparian zones and pine trees in highland locations; agriculture (41%) major row crops of cotton and peanuts; open water (1.5%); and urban areas (12.5%). Soils in the study area are clay, dolostone, and sandstone (Figure 2B), which are underlain by the relatively watertight Hawthorne formation, restricting the movement of groundwater to lower geological layers (Stringfield, 1966), and indicated as the bedrock. The shallow nature of the aquifer and the impermeable Hawthorne formation leads to reported groundwater saturation excess flow (Bosch et al., 2010; Bosch et al., 2017), principally in the riparian areas. Estimated aquifer thickness (m) (Shangguan et al., 2017) (vertical distance between ground surface and bedrock) is presented in Figure 2C. These data illustrate distinct areas of shallow thickness along the riparian corridor.

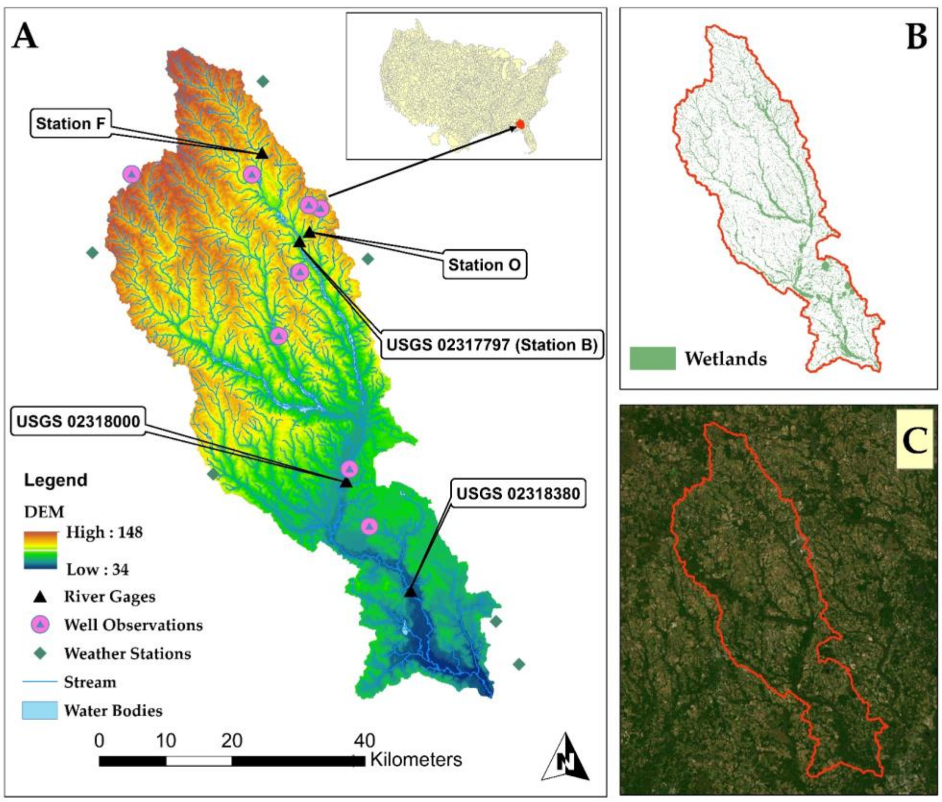

Figure 1. Maps of the Little River Watershed, showing (A) elevation, stream gages, and monitoring wells; (B) wetland delineations (USFWS, 2018); and (C) satellite image, showing riparian areas along the complex channel network.

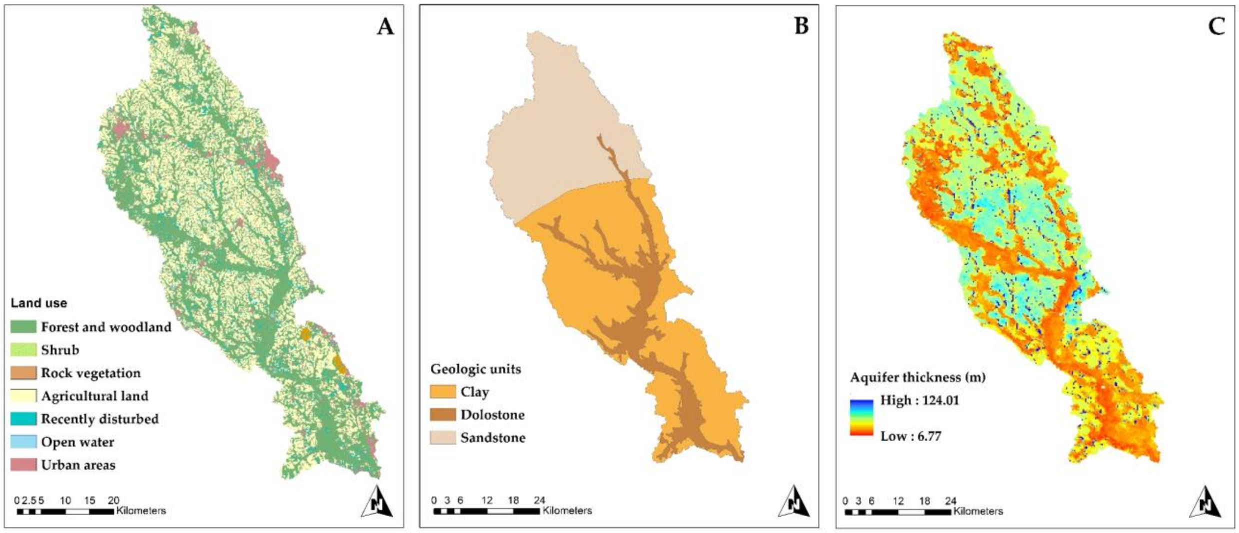

Figure 2. Land use, geologic, and aquifer thickness (m) of the study watershed.

2.2 Hydrologic Model of the Little River Watershed

In this section we outline the hydrologic modeling tool used to address the study objectives. The base model is SWAT+, amended to include the *gwflow* module which simulates groundwater saturated excess flow in a physically based spatially distributed manner.

2.2.1 SWAT+ model

The Soil and Water Assessment Tool (SWAT; Arnold et al., 1998) is a process-based, semi-distributed, continuous-time, basin-scale hydrologic model that has been widely used over the last 25 years (Bieger et al., 2016). The model is often used to predict the enduring effects of land use practices, climate change impact, and non-point source pollution on water resources, sediment, and agricultural chemical yields within river basins. The model segments the watershed into hydrological response units (HRUs) which are computational entities defined by specific values of slope, land use, and soil properties (Neitsch et al. in 2011). Water balances are calculated on a daily time step for the soil profile (HRU), aquifer (HRU), channel (subbasin), and reservoirs. Recently, a restructured version of the SWAT model called SWAT+ was introduced by Bieger et al. (2016). The new version offers enhanced flexibility in linking hydrologic components within a watershed system. Unlike the original SWAT model, which is restricted to a single stream channel per subbasin, SWAT+ allows the simulation of sediment, water, and nutrient movement across numerous channels throughout catchments of varying spatial scale. Within this framework, hydrologic objects comprise reservoirs, stream channels, ponds, wetlands, HRUs, and aquifers.

For this study, the SWAT+ model is constructed for the 2000-2015 period using the datasets listed in Table 1. This model is part of the National Agroecosystem Model (NAM) initiative (Arnold et al., 2020; White et al., 2022), a nationwide endeavor for evaluating conservation policies. Hydrologic features of the SWAT+ model is presented in Table 2, including 1,816 channels (NHD+ stream segments) and 4,844 HRUs.

Table 1. Datasets used to construct the standalone SWAT+ models and the gwflow inputs (Bailey et al., 2023).

	Dataset	Resolution (m)	Source
SWAT+ model	Land use, Land cover	30	U.S. Geological Survey, National Land Cover Data
	Field boundaries		Yan and Roy (2016)
	Topographic slope map	10	USGS National Elevation Dataset (Gesch et al., 2018)
	Weather		Global historical climatology network; PRISM
	Soil boundaries and properties	10	Soil Survey Staff (2014)
	Stream segments		NHD+ Moore and Dewald (2016)
	Crop rotation		USDA–NASS, CDL
	Lakes and reservoirs		Moore and Dewald (2016)
	Water use		Dieter et al. (2018)
	Discharge from facilities		Skinner and Maupin (2019)
Gwflow	Groundwater head	Vector Points	Bailey and Alderfer (2022)
	Aquifer thickness	250	Shangguan et al. (2017)
	Tile drainage	30	Valayamkunnath et al. (2020)
	Geologic units	Vector Polygons	Horton et al. (2017)

Table 2. Characteristics for the study watershed.

						mm	km^2	*gwflow* grid		
Watershed	State	HUC2 Region	HUC8	# Channels	# HRU	Annual Precip.	Area	Rows	Cols	Cell size (m)
Little River	GA	South Atlantic-Gulf	03110204	1816	4844	1287	2309	197	120	500

2.2.2 *gwflow* module

We modified the base SWAT+ model to include the *gwflow* module for groundwater modeling and groundwater interaction with hydrologic objects within the watershed. The *gwflow* module, developed by Bailey et al. (2020), has been included into SWAT+ as an optional subroutine and serves as alternative to the original groundwater module. This addition enables physically based spatially distributed modeling of groundwater storage and flow in unconfined aquifer systems. The *gwflow* module employs a collection of grid cells, also known as aquifer control volumes, to model the storage and movement of groundwater (Figure 3). The thickness of each cell is equivalent to the thickness of the aquifer, extending from the ground surface to the bedrock. The user specifies the cell size.

Groundwater storage volume V (m^3) is updated during each daily time step (time n to time $n+1$) for each grid cell (i, j) using the following groundwater balance equation:

$$V_{i,j}^{n+1} = V_{i,j}^{n} + (sources_{i,j}^{n} - sinks_{i,j}^{n} \mp lateral\ flow_{i,j}^{n})(t^{n+1} - t^{n}) \quad (1)$$

where sources include stream seepage, lake seepage, and recharge, and sinks include groundwater discharge to streams, saturation excess flow to streams, tile drainage outflow to streams, pumping, groundwater discharge to lakes, and groundwater ET. Recharge is provided by soil percolation from HRUs, using a geographic intersection between grid cells and HRUs. Groundwater exchange with channels and lakes/reservoirs is performed for grid cells that intersect channel and reservoir objects. The calculation of tile drainage outflow, groundwater-stream exchange, and groundwater-lake exchange involves the use of Darcy's Law, which utilizes many object qualities such as streambed conductivity, stream width, and stream length. Lateral flow is Darcy flow between neighboring cells, which uses hydraulic conductivity (K) and saturated thickness specific to each cell and cell-to-cell gradients in hydraulic head h.

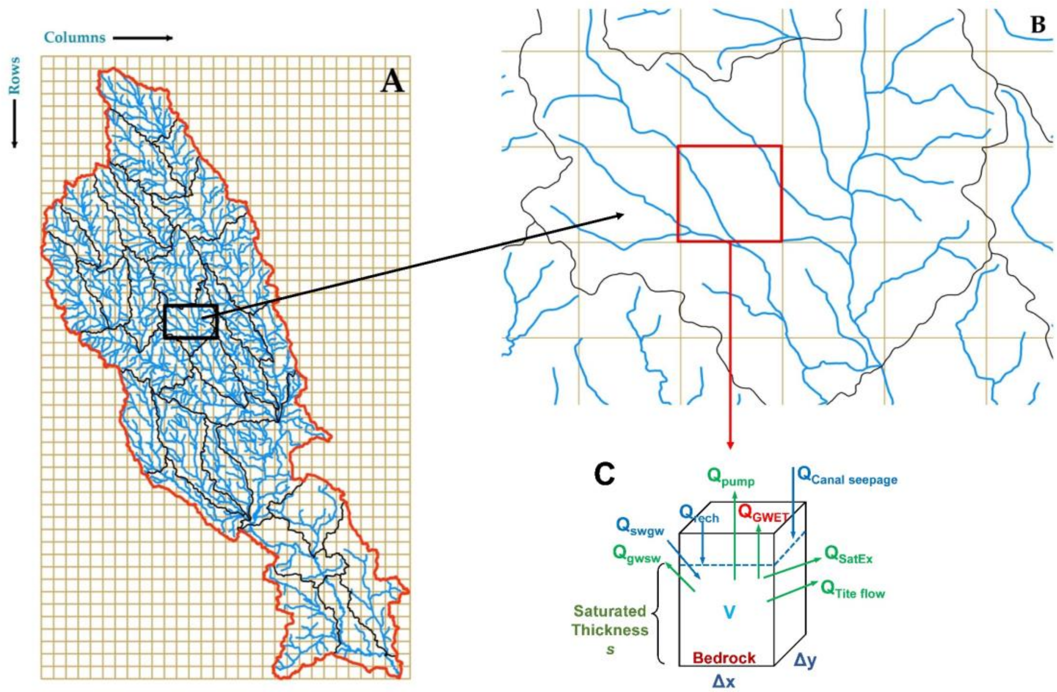

Figure 3. Spatial layout and calculation method of the *gwflow* module within the Little River Watershed, showing (A) grid cells, watershed boundary (red line), stream channels (blue lines), and subbasins (black lines) for the study watershed; (B) close-up of grid and channels; and (C) representing the hydrologic fluxes for each individual cell.

After determining the new volume $V_{i,j}^{n}$, groundwater head is calculated using the specific yield (S_y) of the cell. By incorporating the *gwflow* module, SWAT+ simulates the dynamics of soil, land surface, and channel processes, while the *gwflow* module specifically models subsurface processes (Figure 4) and aquifer-object interactions. Groundwater-induced saturation excess runoff is simulated when the groundwater head h, rises above the elevation of the ground surface. This phenomenon often happens after precipitation events that induce a fast rise in the water table. The volumetric flux (m^3/day) of groundwater excess flow is computed as:

$$Q_{satex} = (h_{i,j} - Z_{surf_{i,j}})(\Delta x \Delta y) S_{y_{i,j}} \quad (2)$$

where h is groundwater head for cell (*i,j*), Z_{surf} is the ground surface elevation for cell (*i,j*), and S_y is specific yield (m^3 water per m^3 of bulk material). The volumetric flow rate Q_{satex} is extracted from the cell and then transferred to the nearest stream channel, within the same day.

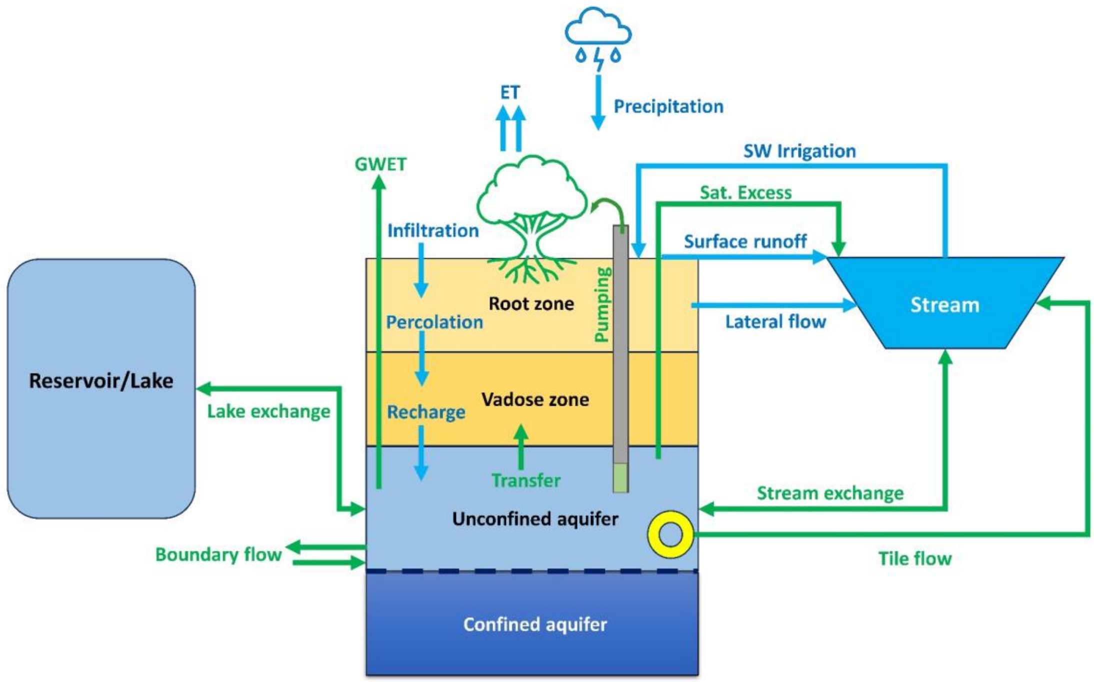

Figure 4. Schematics representation of the hydrologic processes in a typical watershed stream-aquifer system with Saturation Excess Runoff; showing main hydrologic elements and hydrologic processes for SWAT+ and *gwflow*. Green arrows demonstrate fluxes that are simulated by *gwflow*, blue arrows represent fluxes that are simulated by SWAT+.

We note that, under real-world conditions, shallow groundwater enters the soil profile before discharging to the land surface. Within the modeling framework used in this study, however, groundwater in *gwflow* cells is not connected hydrologically to soil water in the SWAT HRUs. While this linkage between the aquifer and the soil profile is included in the *gwflow* module (Yimer et al., 2023), we neglect it here to provide detailed analysis of where groundwater discharge occurs. At a regional scale, we assume that groundwater discharge fluxes will be the same, whether simulated by the *gwflow* subroutine, on a cell basis, or by the soil saturation excess routine of SWAT+, on an HRU basis. We selected a cell size of 500 m (Table 2). The datasets used for populating the cell values in *gwflow* consist of S_y, K, aquifer thickness, and initial groundwater head (see Table 1). For this study, initial head for each cell was estimated by spatial interpolating between USGS monitoring wells (see Figure 1) using values from the year 2000. The identification of cells involved in groundwater-lake exchange and groundwater-channel exchange is achieved by intersecting cells with NHD+ channels and water bodies (Table 1).

2.2.3 Model Calibration and Testing

The SWAT+*gwflow* model has a warm-up period of 2000–2001, a calibration period of 2002–2008, and a testing period of 2009–2015. The SWAT+*gwflow* model is calibrated and tested using the Parameter Estimation Software (PEST; Doherty, 2020). In this work, the objective function (OF) includes monthly streamflow (m^3/sec) obtained from USGS stream gage stations at one river gage location for calibration, and four other gages sites for testing, and average annual groundwater head (m) collected from USGS monitoring wells at ten different locations. The impact of each of these sites on the composite OF was modified by adjusting the weights assigned to the residuals to ensure that each site has a comparable level of importance and relevance in selecting the best parameter values. Monthly simulated streamflow is evaluated using Nash–Sutcliffe Efficiency Index (NSE), Kling–Gupta Efficiency Index (KGE), percent bias (PBIAS), and coefficient of determination (R^2). Annual simulated groundwater head is evaluated using mean absolute error (MAE).

The parameters to be modified by PEST (Table 3) were selected based on the SWAT model documentation and literature (e.g., Koo et al., 2020; Arnold et al., 2013), and focus on surface runoff, evaporation, soil properties, groundwater processes, lateral flow, time of concentration, and channel flow processes.

2.2.4 Addressing Study Objectives

We use the calibrated and tested model to quantify the impact of groundwater saturation excess flow on hydrologic fluxes, streamflow generation, and wetland development and location. To quantify influence on hydrologic fluxes, we compare hydrologic results (runoff, recharge, soil lateral flow, groundwater-channel interactions) from calibrated simulations with and without groundwater saturation excess flow enabled. For streamflow generation, we compute the fraction of streamflow that originates from groundwater saturation excess flow, aggregated and temporally. For wetland development and location, we compare volumetric fluxes of groundwater saturation excess flow spatially to wetland areas, and the frequency of saturation for each cell in the *gwflow* grid as an indicator of wetland persistence.

Table 3. Description and hydrological processes of the selected parameters for the SWAT+*gwflow* model for Little Watershed.

Parameters	Description	Hydrologic Processes
CN2 #	SCS runoff curve number for moisture condition II	Surface runoff processes (cn)
surq_lag	Surface runoff lag time (days)	Time of concentration processes (par)
esco #	Soil evaporation compensation factor	Potential and actual evapotranspiration processes, and percolation (hydro)
epco #	Plant uptake compensation factor	
perco #	Percolation coefficient	
rech_del	Recharge delay (days)	Groundwater flow processes (*gwflow*)
Kaqu #	Aquifer hydraulic conductivity for a specific zone (m/day) for i^{th} zone	
Syaqu #	Aquifer specific yield for a specific zone for i^{th} zone	
bed_k	Streambed hydraulic conductivity (m/day)	
bed_thick	Streambed thickness (m)	
bed_depth	River depth (m)	
tile_depth	Depth of tiles below ground surface (m)	
tile_area	Area of groundwater inflow (m^2) to tile	
tile_k	Hydraulic conductivity of the drain perimeter (m/day)	

ch_n #	Manning's n for the main channels	Channel flow processes (cha)
ch_k #	Effective hydraulic conductivity of the main channels (mm/h)	
awc #	Available water capacity of the soil layer (mm H_2O/mm soil) for i^{th} layer	Soil water processes (sol)

3 Results and Discussion

3.1 Effect of Groundwater Saturation Excess Flow on Hydrologic Fluxes

The comparison between observed and simulated monthly streamflow at five locations (Figure 5, Table S2) shows that simulated monthly discharge considering saturation excess runoff in the hydrologic simulation a significant improvement in term of statistical performance of NSE, R^2, KGE, and PBIAS. For the most downstream gauge (USGS 02318000; Figure 1A), the NSE improves from 0.61 to 0.68 when including saturation excess flow, and the PBIAS improves from 5.8 to -0.5. For Station F, the upstream most gauge in a local area with high wetland density (Figure 1B), the NSE improves from 0.42 to 0.58 (38% increase), and KGE from 0.37 to 0.56.

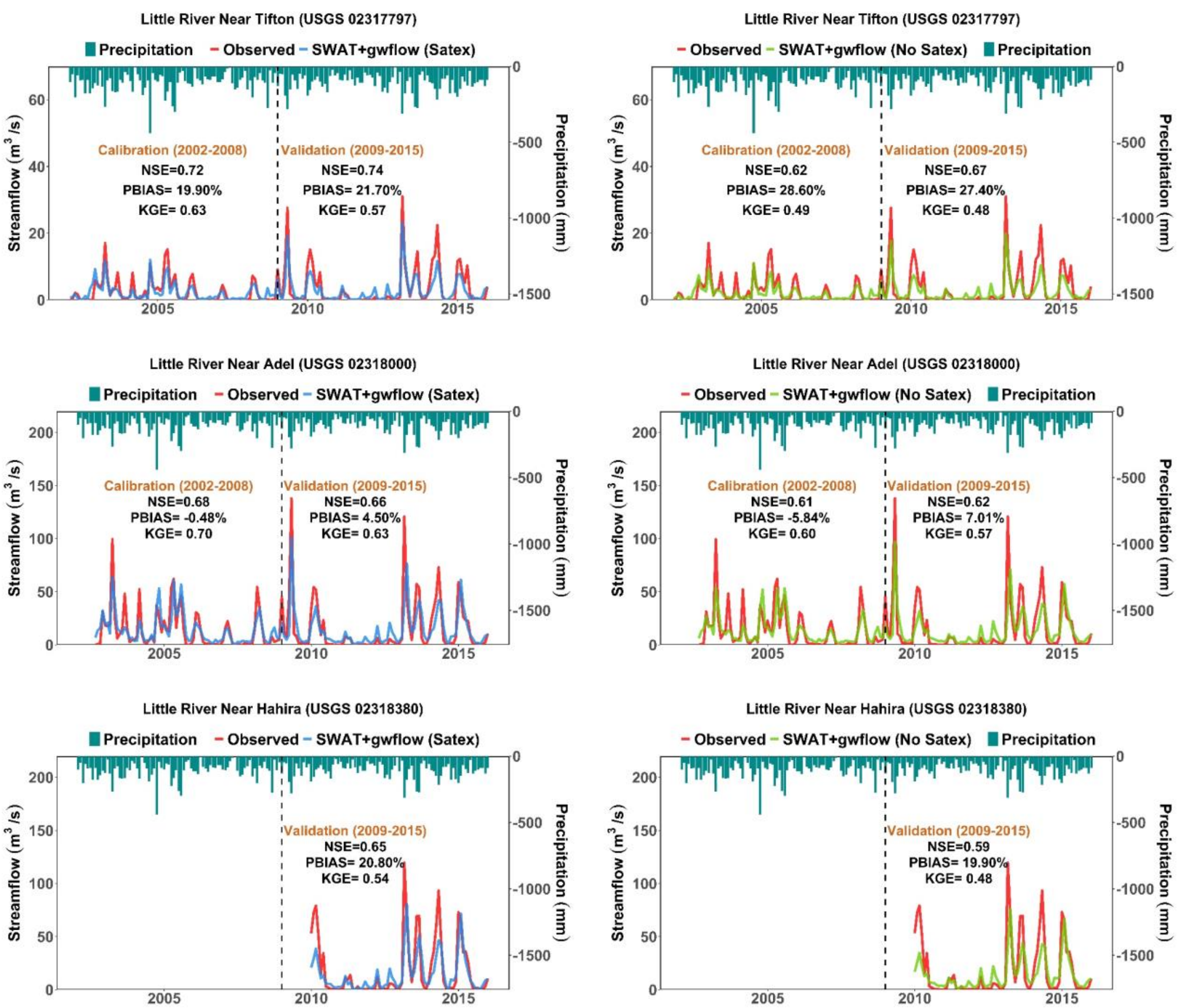

Figure 5. Observed and simulated monthly streamflow for SWAT+*gwflow* model for selected USGS stream gaging sites within the study watershed for two scenarios: minimizing streamflow

considering saturation excess runoff [left column] and minimizing streamflow without saturation excess runoff [right column]. Performance statistics (NSE, PBIAS, KGE) are shown for each gage site.

The improvement in streamflow estimation is due to the higher overall water yield generated when including saturation excess flow. As seen in Table 4, water yield when including vs. excluding saturation excess flow is 324 mm/year (for a yield fraction of 0.25) and 296 mm/year respectively. Of the 324 mm/year, approximately half (163 mm/year) is from groundwater saturation excess flow, resulting in a baseflow fraction of 41%. When groundwater saturation excess flow is not considered in the simulation, the PEST seeks to compensate (i.e., minimize the difference between observed and simulated streamflow) by increasing tile drainage flow and surface runoff. Nevertheless, the resulting water yield (295 mm) does not achieve the correct magnitude of water yield (i.e., 324 mm). It is interesting to note that, rather than increasing groundwater discharge via the channel bed by increasing channel bed hydraulic conductivity, tile drainage outflow was increased.

Table 4. Average annual hydrologic fluxes (mm) for the study watershed and key hydrologic fractions for the two calibration scenarios (with/without groundwater saturation excess flow). Groundwater discharge = groundwater flowing into channel across channel bed.

	Flux (mm)	Minimizing Streamflow (SatEx)	Minimizing Streamflow (No SatEX)
Input	Precipitation	1310.2	1310.2
	Boundary Outflow	1.1	1.5
Watershed Output	ET	953	957
	Surface Runoff	171	184
	Soil Lateral Flow	20	17
	Stream seepage	35	4.8
	Groundwater discharge	0	7.2
	Saturation Excess Flow	163	0
	Tile flow	6	92
Internal Flows	Recharge	138	126
	Pumping Irrigation	0.00	0.00
	GW-Lake Outflow	1.2	0.06
	Surface Water Irrigation	0.00	0.00
Fractions	Water Yield [a]	**324**	**296**
	ET Fraction [b]	0.72	0.73
	Baseflow Fraction [c]	**0.41**	**0.32**
	Yield Fraction [d]	0.25	0.23
	Recharge Fraction [e]	0.11	0.10

a: Water Yield = Surface Runoff + Lateral Flow + Groundwater discharge - Stream seepage + Saturation Excess Flow + Tile flow
b: ET / Precipitation
c: Net groundwater inflow to streams (Stream Seepage + Sat Excess Flow+ Tile flow) / Water Yield
d: Water Yield / Precipitation
e: Recharge / Precipitation

Monthly groundwater saturation excess flow is shown in Figure 6 for both the watershed and groundwater systems. System inputs (precipitation, boundary inflow) are displayed as positive values, whereas system outputs (tile drainage, runoff, groundwater saturation excess flow, surface ET, and lateral flow) are displayed as negative values. Groundwater saturation excess flow fluctuates seasonally, based on incoming recharge from rainfall events. On an annual basis, the fraction of water yield that is groundwater saturation excess flow ranges from 0.29 (2002) to 0.58 (2011) (Figure 7A).

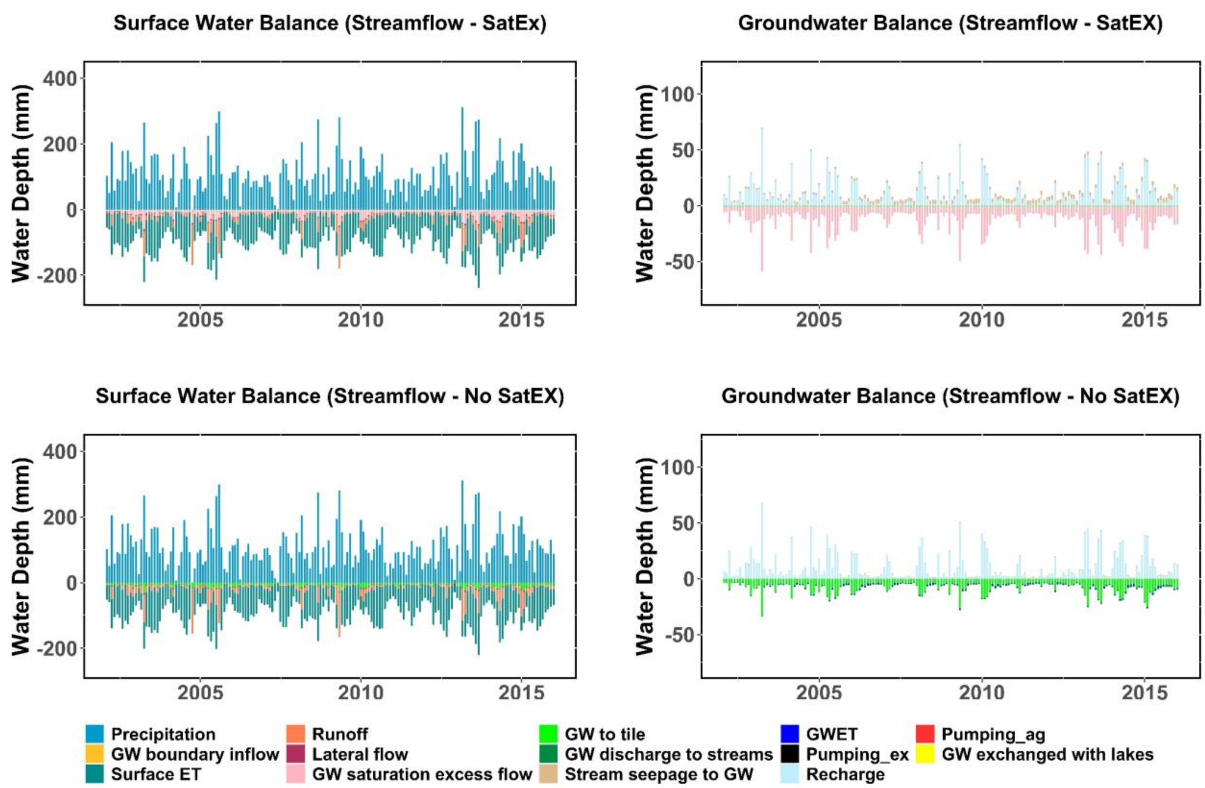

Figure 6. Monthly surface water fluxes (mm) [left column], and groundwater fluxes (mm) [right column] for the simulation period of (2002–2015) for four scenarios of Little Watershed.

Typically, years of high groundwater saturation excess fractions correspond to years of low rainfall. For example, rainfall for 2007 (saturation excess fraction = 0.51) was 987 mm (compared to 1,310 mm/year average), and rainfall for 2011 (saturation excess fraction = 0.58) was 959 mm/year. This is due to antecedent groundwater conditions, as high groundwater levels generated during previous years intersect the ground surface during the following years, producing high flows as compared to runoff and soil lateral flow. This is also demonstrated by comparing annual fluxes (runoff, soil lateral flow, groundwater saturation excess flow) to annual rainfall (Figure 7C), with groundwater saturation excess flow exhibiting a much weaker relationship to rainfall, due to the impact of antecedent conditions.

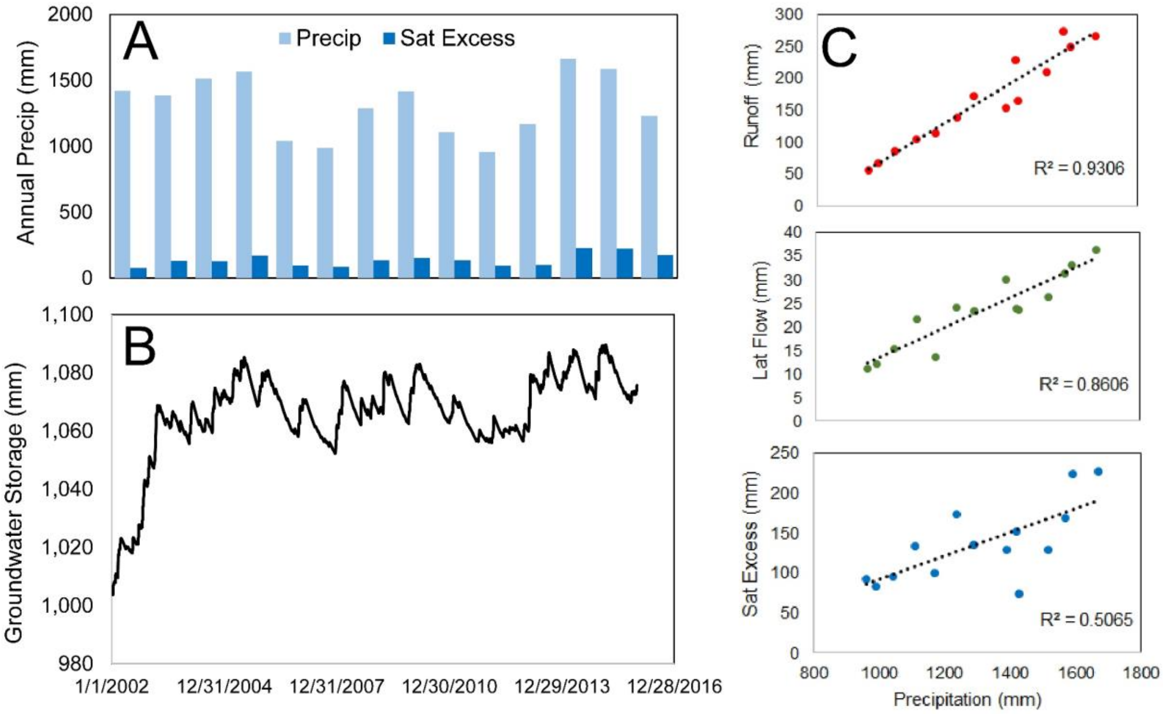

Figure 7. (A) annual precipitation (mm) and groundwater saturation excess flow (mm); (B) daily total groundwater storage (mm), normalized to watershed area; (C) 1:1 relationships between annual basin precipitation and hydrologic fluxes (runoff, soil lateral flow, groundwater saturation excess flow).

3.2 Effect of Groundwater Saturation Excess Flow on Aquifer Features and Fluxes

Table S3 lists the MAE of groundwater monitoring wells (10 locations) for the two calibration scenarios. MAE results demonstrate a significant improvement (average MAE = 1.84 m) compared to excluding groundwater saturation excess flow (MAE = 3.48 m). Nevertheless, a few locations have greater error, although these residuals are small compared to the saturated thickness of the aquifer. Figure 8 compares annual observed and simulated groundwater heads for both calibration scenarios. Including groundwater saturation excess flow improves the simulated groundwater head fluctuation at most locations. Without groundwater saturation excess flow, groundwater head rises above the ground surface, but with no mechanisms to release groundwater to runoff. Groundwater responds to near-surface hydrology of rainfall, ET, soil percolation and recharge, although this response can be delayed due to antecedent groundwater storage conditions (see Figure 7C, relationship between precipitation and groundwater saturation excess flow).

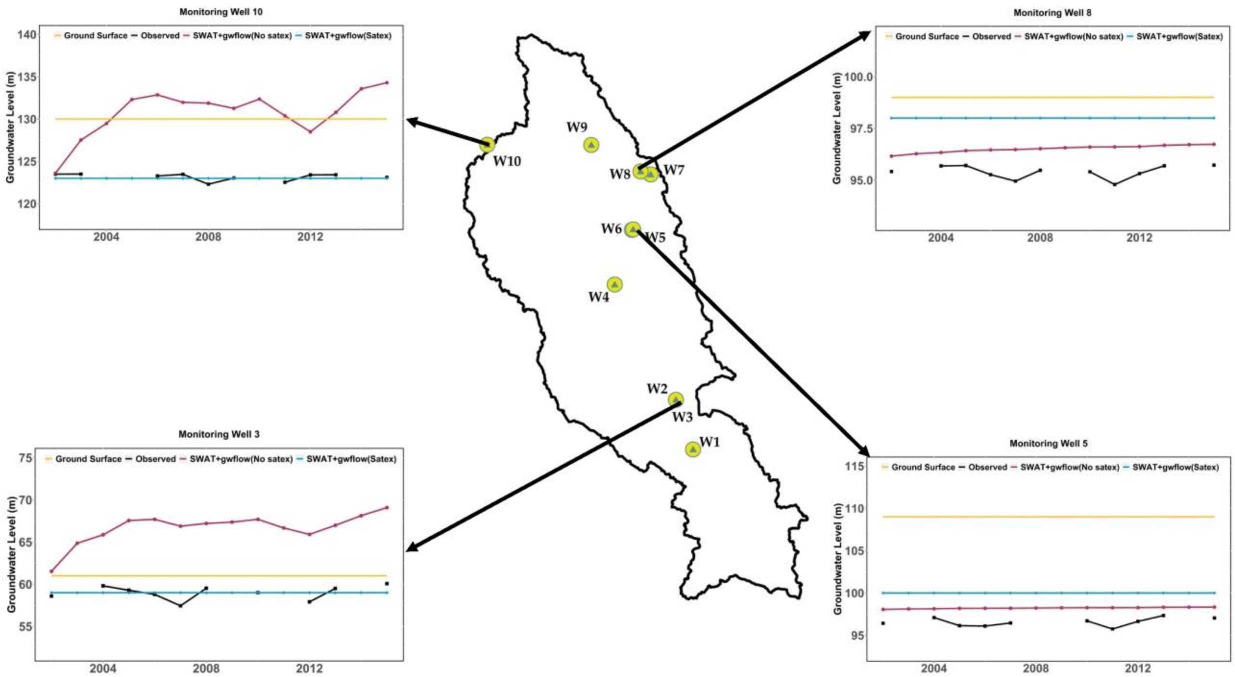

Figure 8. Maps of mean absolute error (MAE) (m) for a selected USGS groundwater monitoring well locations for the simulation period of (2002–2015) for scenarios minimizing streamflow.

The influence of groundwater saturation excess flow on groundwater fluxes can be shown spatially (Figure 9). Using cell-by-cell differences for the year 2015, saturated thickness (m) and groundwater head (m) are much lower when including groundwater saturation excess flow, due to the release of high groundwater to streams; groundwater recharge is much higher (purple color) in areas between streams; and groundwater discharge via channel bed is lower. Over the simulation period, recharge is higher when including groundwater saturation excess flow (138 mm) than excluding (126 mm). In the exclusion simulation, surface runoff is increased in an attempt to increase streamflow to match measured values; increasing surface runoff decreases infiltration and soil percolation, which in turns decreases recharge to the water table. This results in a local lowering of groundwater head, in relation to the inclusion simulation.

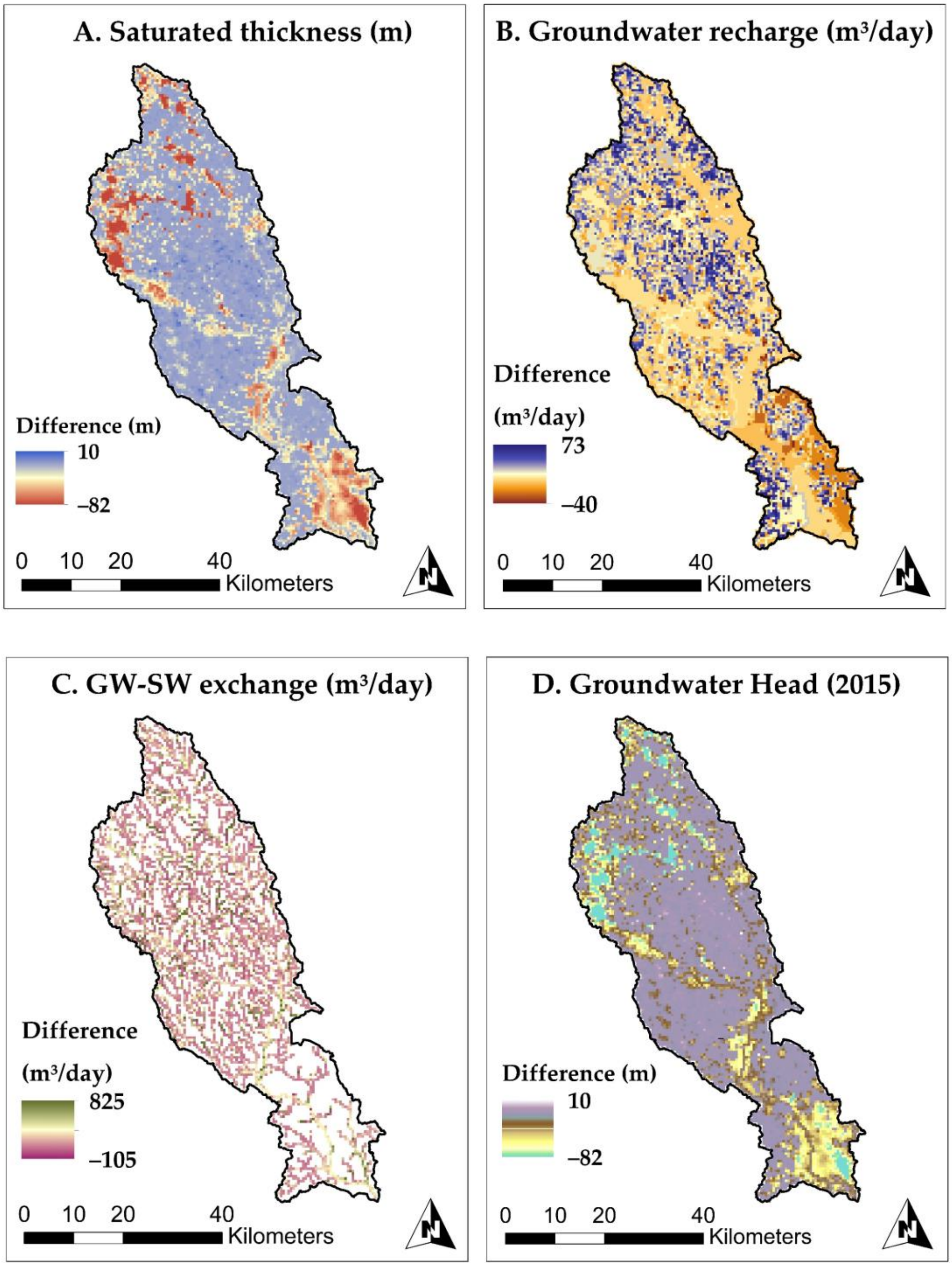

Figure 9. Difference maps between hydrologic simulation considering saturation excess flow and hydrologic simulation without saturation excess flow for (a) saturated thickness (m) for year 2015; (b) average annual recharge flow (m^3/day) for year 2015; (c) average annual groundwater-stream exchange rate (m^3/day) for year 2015; and (d) final (end of year 2015) groundwater head (m).

To elucidate temporal dynamics of groundwater saturation excess flow, we analyze daily time series rainfall, recharge, groundwater volume, and groundwater saturation excess flow for two years (2002-2003) (Figure 10). These time series demonstrate the response of groundwater storage to rainfall-induced recharge, which in turn leads to groundwater saturation excess flow in many local areas of the watershed. We note that groundwater saturation excess flow responds temporally in a like manner to runoff, indicating its strong dependence on short-term rainfall events that raise the water table to the ground surface. Figure 11 shows spatially the impact of two rainfall periods (10/27/2002 to 11/14/2002; 2/18/2003 to 3/8/2003) on groundwater head and groundwater saturation excess flow. Local areas of high increases in groundwater head, due to rainfall-induced recharge, produce local areas of groundwater saturation excess flow. These results emphasize the need to include groundwater saturation excess flow in hydrological modeling for watersheds with shallow groundwater.

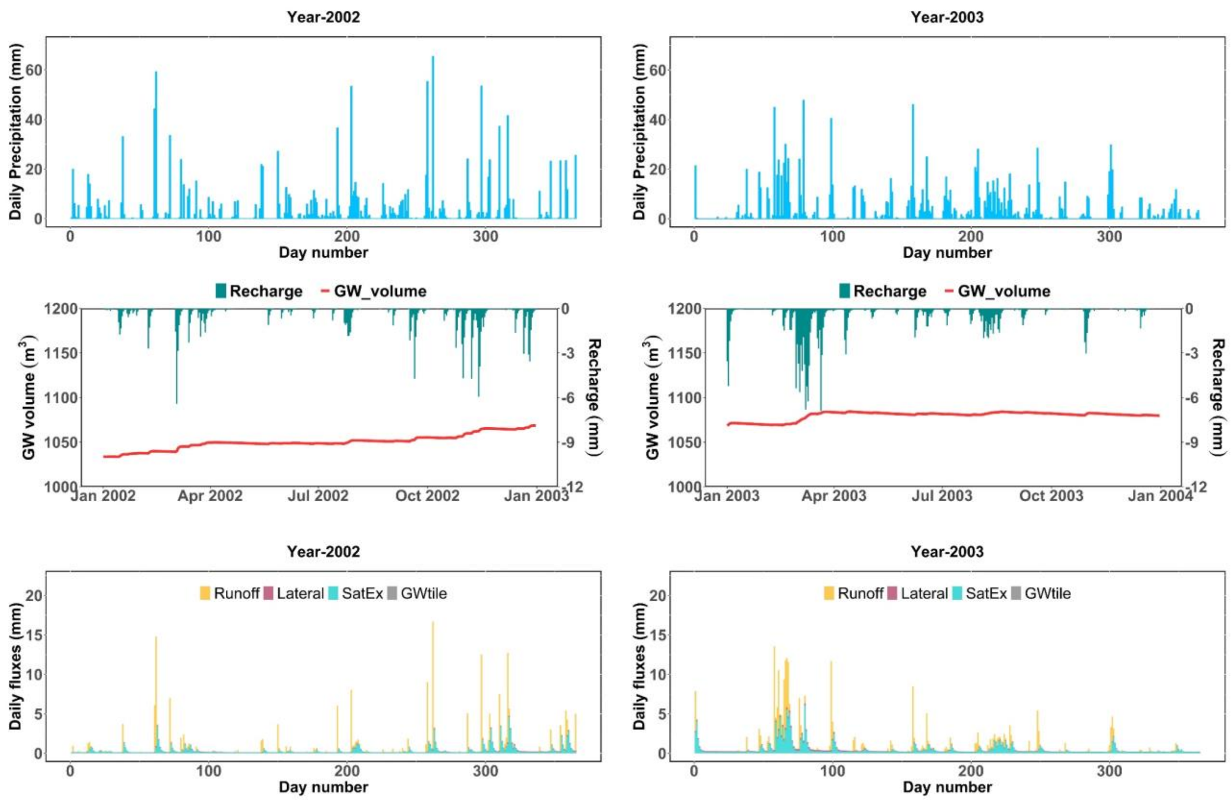

Figure 10. Average daily basin precipitation, groundwater volume, recharge, and streamflow components for the years 2002 [left column] and 2003 [right column].

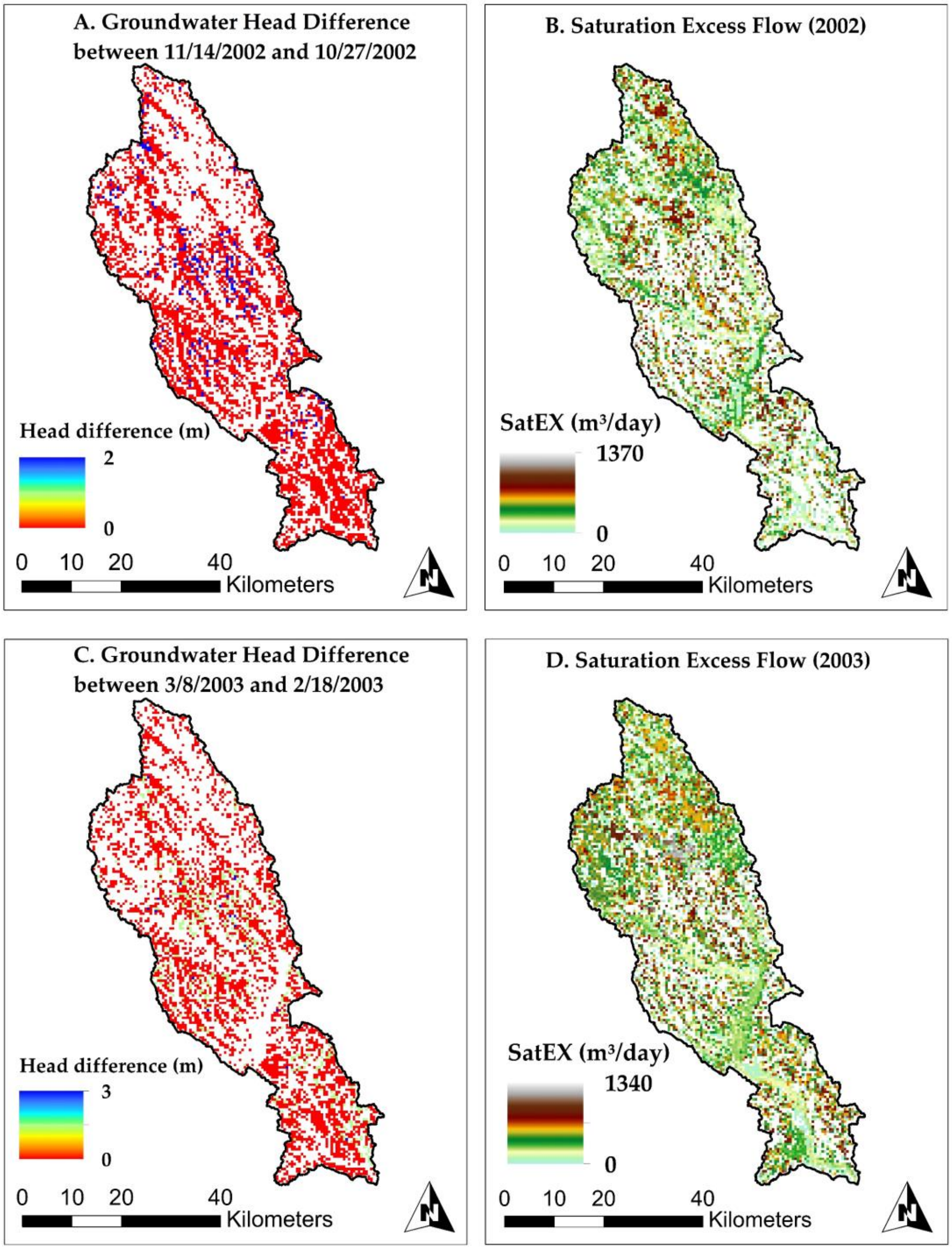

Figure 11. Maps represent (a) groundwater head difference (11/14/2002; during storm) and (10/27/2002; before storm); (b) average daily saturation excess flow (m^3/day) for the year 2002; (c) groundwater head difference (3/8/2003; during storm) and (2/18/2003; before storm); and (d) average daily saturation excess flow (m^3/day) for the year 2003.

3.3 Effect of Groundwater Saturation Excess on Wetland Development

Groundwater saturation excess runoff is key to wetland development and vegetation as it offers a continuous or near-continuous source of water and nutrients. Although our approach does not explicitly simulate wetland objects within the hydrologic model, we can use the model results to indicate locations of likely wetland development, based on timing and magnitude of groundwater saturation excess runoff. A similar approach was used by Feinstein et al. (2019) in delineating fen locations and comparing these locations with mapped fens for a 223 km^2 basin in southeastern Wisconsin, USA, although under steady state groundwater conditions.

Raster maps of simulated daily average rates (m^3/day) of groundwater saturation excess flow are overlain by watershed wetlands (see Figure 1B) for years of low flux (2007) and high flux (2013) (Figure 12A, B) based on annual groundwater saturation excess flow (Figure 12E), showing the influence of timing on flux rates. The close comparison of wetland locations and saturation excess flow (Figure 12F; year 2013) reveals that wetland development is often more naturally pronounced in regions where the water table periodically rises to the ground surface. By spatial joining saturation excess flow rates to wetland areas, we show that there are relationships between the size of the wetland and the amount of simulated groundwater saturation excess flow (Figure 12C, D).

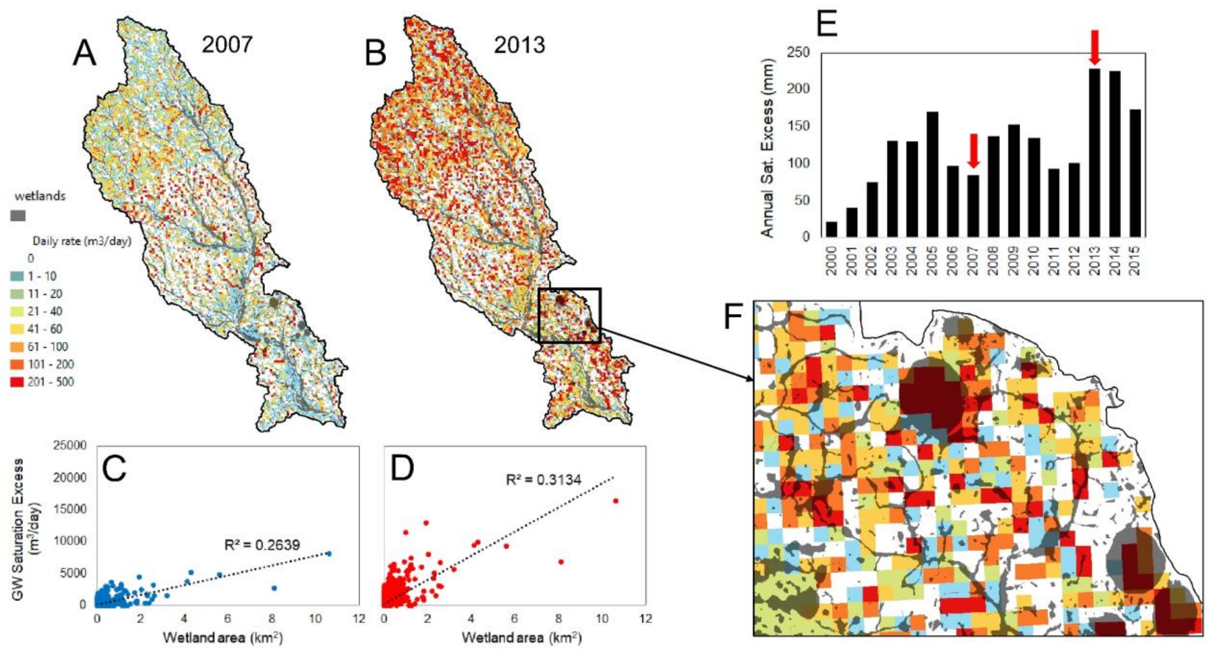

Figure 12. Maps represent (A) average daily saturation excess flow (m^3/day) for the year 2007 (dry year) with wetland areas; (B) average daily saturation excess flow (m^3/day) for the year 2013 (wet year) with wetlands areas; (C) relationship between groundwater saturation excess runoff and wetland area for the year 2007; (D) relationship between groundwater saturation excess runoff and wetland area for the year 2013; (E) basin average annual saturation excess flow (mm); and (F) zoomed region of wetland and cell-by-cell saturation excess runoff flux for the year 2013.

Finally, we show the fraction of time (over the 16-year simulation period, 2000-2015) that each cell experiences groundwater saturation excess flow (Figure 13) and relate this fraction to wetland locations. Although 71% of the watershed area experiences groundwater saturation excess flow less than 20% of the time, many local areas (9% of watershed area) experience flow more than 80% of the time (Figure 14). The locations that are saturated more than 80% of the time cover a spatial area of 539 km^2 (2,155 grid cells, each with a spatial area of 500 m x 500 m = 250,000 m^2). This area corresponds well to the 399 km^2 covered by the delineated wetlands. From these results we conclude that this modeling approach can simulate, in a physically based manner, the locations and quantities of a necessary groundwater source for wetlands and other groundwater-dependent ecosystems.

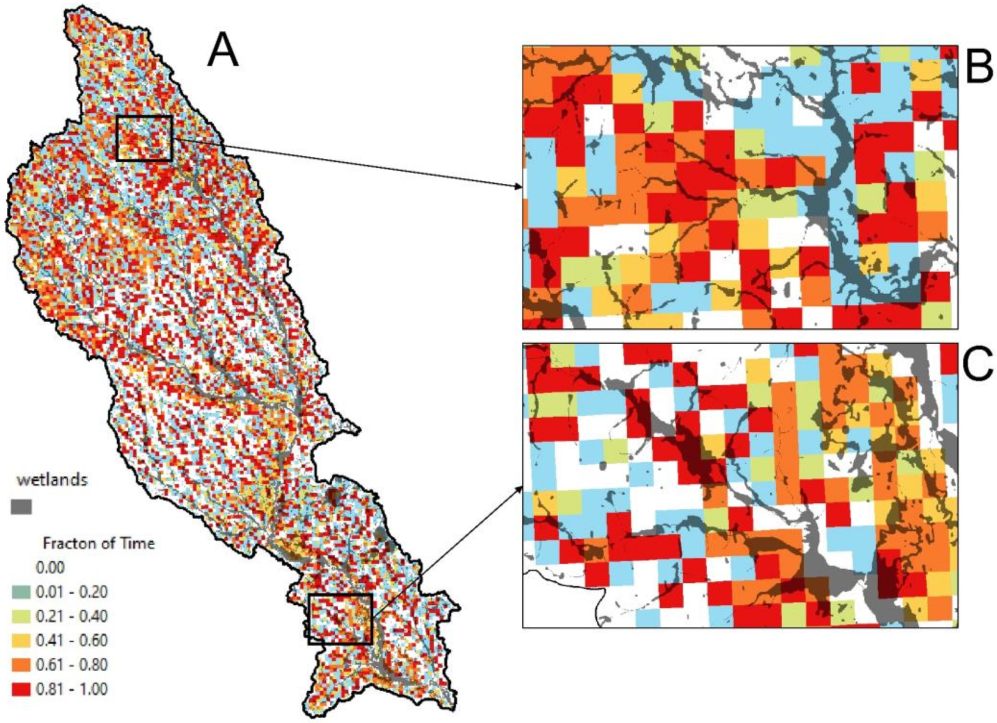

Figure 13. (A) Map of fraction of time saturated during the 2000-2015 simulation period overlain by mapped wetland areas, showing two local areas (B, C).

The model could therefore be used as a tool to quantify the impact of system changes on these locations and quantities, providing insight into the sustainability of wetlands in the face of changes in climate, land use, population, and management practices. To provide a more physically realistic modeling approach and model wetland development and evolution explicitly, the modeling approach presented here could be further developed by implementing wetland objects, a current option in SWAT+, and setting groundwater saturation excess flow as inflow to these objects. Outflow from wetlands would then be added to streams, thereby providing important timing of streamflow generation.

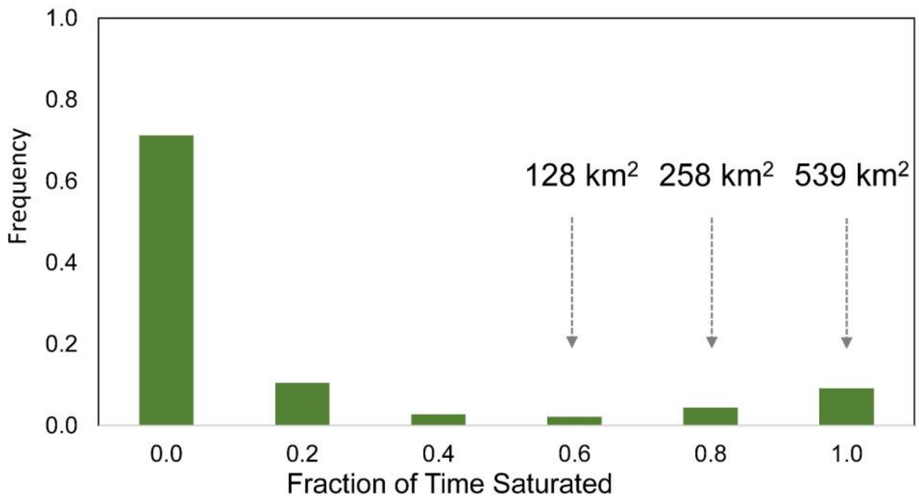

Figure 14. Histogram of fraction of time that land surface is saturated in the study area.

4 Summary and Conclusions

In this article, we use a surface–groundwater hydrologic modeling approach with physically based spatially distributed groundwater storage and flow modeling (SWAT+*gwflow*) to represent the mechanism of groundwater saturation excess flow. We apply the approach to a humid, low-gradient watershed, the Little River Watershed in Georgia, USA and investigate its impact on hydrologic features and fluxes. Upon model calibration and testing, we analyze model results to quantify the impact of groundwater saturation excess flow on surface hydrologic fluxes, groundwater fluxes, and the generation of source water for wetlands. From the results, we conclude the following:

1. Including groundwater saturation excess flow in a watershed model can improve the estimation of streamflow generation, for the right reasons. Without this process included, automated calibration procedures (e.g., PEST, as used in this study) attempt to compensate by altering other hydrologic fluxes to unrealistic magnitudes, to match measured streamflow. In this study, tile drainage outflow was increased dramatically, even though tile drainage is not a prevalent cultivation practice in the watershed. Also, surface runoff was increased to match streamflow, thereby decreasing recharge to the water table.
2. Groundwater saturation excess flow plays a key role in governing hydrologic behavior of the watershed. Rainfall-induced recharge raises groundwater levels on a short temporal scale, leading to flashy streamflow on the same time scale as surface runoff.
3. The fraction of streamflow that originates from groundwater saturation excess flow ranges from 0.29 to 0.58, during the 2002-2015 period. Years with high fractions typically have lower annual rainfall, indicating the influence of antecedent groundwater storage conditions. Due to this influence, groundwater saturation excess flow has a weak correlation to annual rainfall as compared to surface runoff and soil lateral flow.

4. Locations of persistent predicted groundwater saturation excess flow correspond to observed locations of wetlands. The hydrologic model can be used to quantify the impact of system changes (climate, land use, management practices) on groundwater saturation excess flow and, through association, the presence and persistence of wetlands.

Acknowledgments

This work was funded by the United State Department of Agriculture–Agricultural Research Service through Cooperative Agreements 59-3098-8-002 and 59-3098-2-001. USDA is an Equal Opportunity Employer and Provider.

Author contributions

R.B., S.A., and J.A. designed the research; R.B., and J.A. performed model coding; R.B., S.A., J.A., and M.W. performed the research; S.A., and R.B. analyzed the data; R.B., and S.A. wrote the paper.

Data Availability Statement

All hydrologic simulations for SWAT+*gwflow* for the Little River Watershed, GIS arrays of models outputs, R codes for plots are available at (https://doi.org/10.5281/zenodo.10079906).

References

Abbas, S., & Xuan, Y. (2019). Development of a new quantile-based method for the assessment of regional water resources in a highly-regulated river basin. *Water Resources Management*, **33**, 3187-3210. https://doi.org/10.1007/s11269-019-02290-z

Aldous, A., & Bach, L. (2014). Hydro-ecology of groundwater-dependent ecosystems: applying basic science to groundwater management. *Hydrological Sciences Journal*, **59**(3-4), 530-544. https://doi.org/10.1080/02626667.2014.889296

Arnold, J., Kiniry, J., Srinivasan, R., Williams, J., Haney, E., & Neitsch, S. (2013). Soil & Water Assessment Tool: Input/output documentation. version 2012. Texas Water Resources Institute 2013 TR-439. https://swat.tamu.edu/media/69296/swat-io-documentation-2012.pdf

Arnold, J., Srinivasan, R., Muttiah, R., & Williams, J. (1998). Large area hydrologic modeling and assessment part I: Model development. *Journal of the American Water Resources Association*, **34**(1), 73-89. https://doi.org/10.1111/j.1752-1688.1998.tb05961.x

Arnold, J., White, M., Allen, P., Gassman, P., & Bieger, K. (2020). Conceptual Framework of connectivity for a national agroecosystem model based on transport processes and management practices. *Journal of the American Water Resources Association*, **57**(1), 154-169. https://doi.org/10.1111/1752-1688.12890

Bailey, R., Abbas, S., Arnold, J., White, M., Gao, J., & Čerkasova, N. (2023). Augmenting the national agroecosystem model with physically based spatially distributed groundwater modeling. *Environmental Modelling & Software*, **160**, 105589. https://doi.org/10.1016/j.envsoft.2022.105589

Bailey, R., & Alderfer, C. (2022). Groundwater Data in Unconfined Aquifers - conterminous United States. *figshare*. Collection. https://doi.org/10.6084/m9.figshare.c.5918738.v2

Bailey, R., Bieger, K., Arnold, J., & Bosch, D. (2020). A new physically-based spatially-distributed groundwater flow module for SWAT+. *Hydrology*, **7**(4), 75. https://doi.org/10.3390/hydrology7040075

Bari, M., Smith, N., Ruprecht, J., & Boyd, B. (1996). Changes in streamflow components following logging and regeneration in the southern forest of Western Australia. *Hydrological Processes*, **10**(3), 447-461. https://doi.org/10.1002/(SICI)1099-1085(199603)10:3<447::AID-HYP431>3.0.CO;2-1

Batelaan, O., De Smedt, F., & Triest, L. (2003). Regional groundwater discharge: phreatophyte mapping, groundwater modelling and impact analysis of land-use change. *Journal of Hydrology*, **275**(1-2), 86-108. https://doi.org/10.1016/S0022-1694(03)00018-0

Bear, J. (1972). Dynamics of fluids in porous media–American Elsevier pub. *Comp., inc. New York, 764p*.

Beaugendre, H., Ern, A., Esclaffer, T., Gaume, E., Ginzburg, I., & Kao, C. (2006). A seepage face model for the interaction of shallow water tables with the ground surface: Application of the obstacle-type method. *Journal of Hydrology*, **329**(1-2), 258-273. https://doi.org/10.1016/j.jhydrol.2006.02.019

Beven, K. (1989). Interflow. In *Unsaturated flow in hydrologic modeling: Theory and practice* (pp. 191-219). Dordrecht: Springer Netherlands.

Bieger, K., Arnold, J., Rathjens, H., White, M., Bosch, D., Allen, P., *et al.* (2016). Introduction to SWAT+, a completely restructured version of the soil and water assessment tool. *Journal of the American Water Resources Association*, **53**(1), 115-130. https://doi.org/10.1111/1752-1688.12482

Bizhanimanzar, M., Leconte, R., & Nuth, M. (2019). Modelling of shallow water table dynamics using conceptual and physically based integrated surface-water–groundwater hydrologic models. *Hydrology and Earth System Sciences*, **23**(5), 2245-2260. https://doi.org/10.5194/hess-23-2245-2019

Bosch, D., Arnold, J., Allen, P., Lim, K., & Park, Y. (2017). Temporal variations in baseflow for the Little River experimental watershed in South Georgia, USA. *Journal of Hydrology: Regional Studies*, **10**, 110-121. https://doi.org/10.1016/j.ejrh.2017.02.002

Bosch, D., Arnold, J., Volk, M., & Allen, P. (2010). Simulation of a low-gradient coastal plain watershed using the SWAT landscape model. *Transactions of the ASABE*, **53**, 1445–1456. https://doi.org/10.13031/2013.34899

Bosch, D., Sheridan, J., & Lowrance, R. (1996). Hydraulic gradients and flow rates of a shallow coastal plain aquifer in a forested riparian buffer. *Transactions of the ASABE*, **39**(3), 865-871. https://doi.org/10.13031/2013.27571

Bosch, D., Sheridan, J., Lowrance, R., Hubbard, R., Strickland, T., Feyereisen, G., & Sullivan, D. (2007). Little river experimental watershed database. *Water Resources Research*, **43**(9). https://doi.org/10.1029/2006WR005844

Brown, J., Bach, L., Aldous, A., Wyers, A., & DeGagné, J. (2010). Groundwater-dependent ecosystems in Oregon: An assessment of their distribution and associated threats. *Frontiers in Ecology and the Environment*, **9**(2), 97-102. https://doi.org/10.1890/090108

Cloke, H., Renaud, J., Claxton, A., McDonnell, J., Anderson, M., Blake, J., & Bates, P. (2003). The effect of model configuration on modelled hillslope–riparian interactions. *Journal of Hydrology*, **279**(1-4), 167-181. https://doi.org/10.1016/S0022-1694(03)00177-X

Deitchman, R., & Loheide, S. (2009). Ground-based thermal imaging of groundwater flow processes at the seepage face. *Geophysical Research Letters*, **36**(14). https://doi.org/10.1029/2009GL038103

Dekker, S., Barendregt, A., Bootsma, M., & Schot, P. (2005). Modelling hydrological management for the restoration of acidified floating fens. *Hydrological Processes*, **19**(20), 3973-3984. https://doi.org/10.1002/hyp.5864

Dieter, C., Maupin, M., Caldwell, R., Harris, M., Ivahnenko, T., Lovelace, J., Barber, N., & Linsey, K. (2018). *Water availability and use science program: Estimated use of water in the United States in 2015* (Circular 1441). US Geological Survey. https://doi.org/10.3133/cir1441

Doherty, J. (2020). PEST, Model-independent Parameter Estimation: User Manual (seventh ed.). *Watermark Numerical Computing, Brisbane, Australia, 3338*, 3349.

Du, T., Hyongki, L., Bui, D., Graham, L., Darby, S., Pechlivanidis, I., *et al.* (2022). Streamflow prediction in highly regulated, transboundary watersheds using multi-basin modeling and remote sensing imagery. *Water Resources Research*, **58**(3), e2021WR031191. https://doi.org/10.1029/2021WR031191

Easton, Z., Fuka, D., Walter, M., Cowan, D., Schneiderman, E., & Steenhuis, T. (2008). Re-conceptualizing the soil and water assessment tool (SWAT) model to predict runoff from variable source areas. *Journal of Hydrology*, **348**, 279– 291. https://doi.org/10.1016/j.jhydrol.2007.10.008

Feinstein, D., Hart, D., Gatzke, S., Hunt, R., Niswonger, R., & Fienen, M. (2019). A simple method for simulating groundwater interactions with fens to forecast development effects. *Groundwater*, **58**(4), 524-534. https://doi.org/10.1111/gwat.12931

Gesch, D., Evans, G., Oimoen, M., & Arundel, S. (2018). The national elevation dataset (pp. 83–110). American Society for Photogrammetry and Remote Sensing.

Gyamfi, C., Ndambuki, J., & Salim, R. (2016). Hydrological responses to land use/cover changes in the Olifants Basin, South Africa. *Water*, **8**(12), 588. https://doi.org/10.3390/w8120588

Hoang, L., Schneiderman, E., Moore, K., Mukundan, R., Owens, E., & Steenhuis, T. (2017). Predicting saturation-excess runoff distribution with a lumped hillslope model: SWAT-HS. *Hydrological Processes*, **31**(12), 2226-2243. https://doi.org/10.1002/hyp.11179

Hunt, R., Krabbenhoft, D., & Anderson, M. (1996). Groundwater inflow measurements in wetland systems. *Water Resources Research*, **32**(3), 495-507. https://doi.org/10.1029/95WR03724

Inamdar, S., Sheridan, J., Williams, R., Bosch, D., Lowrance, R., Altier, L., & Thomas, D. (1999). Riparian ecosystem management model (REMM): I. Testing of the hydrologic component for a coastal plain riparian system. *Transactions of the ASAE*, **42**(6), 1679-1690. https://doi.org/10.13031/2013.13332

Kazmierczak, J., Müller, S., Nilsson, B., Postma, D., Czekaj, J., Sebok, E., *et al.* (2016). Groundwater flow and heterogeneous discharge into a seepage lake: Combined use of physical methods and hydrochemical tracers. *Water Resources Research*, **52**(11), 9109-9130. https://doi.org/10.1002/2016WR019326

Kløve, B., Ala-Aho, P., Bertrand, G., Boukalova, Z., Ertürk, A., Goldscheider, N., *et al.* (2011). Groundwater dependent ecosystems. Part I: Hydroecological status and trends. *Environmental Science & Policy*, **14**(7), 770-781. https://doi.org/10.1016/j.envsci.2011.04.002

Koo, H., Chen, M., Jakeman, A., & Zhang, F. (2020). A global sensitivity analysis approach for identifying critical sources of uncertainty in non-identifiable, spatially distributed environmental models: A holistic analysis applied to SWAT for input datasets and model parameters. *Environmental Modelling & Software*, **127**, 104676. https://doi.org/10.1016/j.envsoft.2020.104676

Mengistu, D., Bewket, W., Dosio, A., & Panitz, H. J. (2021). Climate change impacts on water resources in the Upper Blue Nile (Abay) river basin, Ethiopia. *Journal of Hydrology*, **592**, 125614. https://doi.org/10.1016/j.jhydrol.2020.125614

Moore, R., and Dewald, T. (2016). The road to nhdp lus — advancements in digital stream networks and associated catchments. *Journal of the American Water Resources Association*, **52**(4), 890-900. https://doi.org/10.1111/1752-1688.12389

Neitsch, S., Arnold, J., Kiniry, J., & Williams, J. (2011). *Soil and Water Assessment Tool Theoretical Documentation version 2009*. Texas Water Resources Institute. https://swat.tamu.edu/media/99192/swat2009-theory.pdf

Rath, P., Bresciani, E., Zhu, J., & Befus, K. (2023). Numerical analysis of seepage faces and subaerial groundwater discharge near waterbodies and on uplands. *Environmental Modelling & Software*, 105828. https://doi.org/10.1016/j.envsoft.2023.105828

Rathjens, H., Oppelt, N., Bosch, D., Arnold, J., & Volk, M. (2015). Development of a grid-based version of the SWAT landscape model. *Hydrological Processes*, **29**, 900–914. https://doi.org/10.1002/hyp.10197

Ruprecht, J., & Schofield, N. (1989). Analysis of streamflow generation following deforestation in southwest Western Australia. *Journal of Hydrology*, **105**(1-2), 1-17. https://doi.org/10.1016/0022-1694(89)90093-0

Sampath, P., Liao, H., Curtis, Z., Herbert, M., Doran, P., May, C., *et al.* (2016). Understanding fen hydrology across multiple scales. *Hydrological Processes*, **30**(19), 3390-3407. https://doi.org/10.1002/hyp.10865

Scudeler, C., Paniconi, C., Pasetto, D., & Putti, M. (2017). Examination of the seepage face boundary condition in subsurface and coupled surface/subsurface hydrological models. *Water Resources Research*, **53**(3), 1799-1819. https://doi.org/10.1002/2016WR019277

Shangguan, W., Hengl, T., Mendes de Jesus, J., Yuan, H., & Dai, Y. (2017). Mapping the global depth to bedrock for land surface modeling. *Journal of Advances in Modeling Earth Systems*, **9**(1), 65-88. https://doi.org/10.1002/2016ms000686

Shedlock, R., Wilcox, D., Thompson, T., & Cohen, D. (1993). Interactions between ground water and wetlands, southern shore of Lake Michigan, USA. *Journal of Hydrology*, **141**(1-4), 127-155. https://doi.org/10.1016/0022-1694(93)90047-D

Sheridan, J. (1997). Rainfall-streamflow relations for coastal plain watersheds. *Applied Engineering in Agriculture*, **13**(3), 333-344. https://doi.org/10.13031/aea.2013.21616.5

Skinner, K., & Maupin, M. (2019). *Point-source nutrient loads to streams of the conterminous United States, 2012* (No. 1101). US Geological Survey. https://doi.org/10.3133/ds1101

Soil Survey Staff (2014). Gridded soil survey geographic (gSSURGO) database for the conterminous United States.

Steenhuis, T., Schneiderman, E., Mukundan, R., Hoang, L., Moges, M., & Owens, E. (2019). Revisiting SWAT as a saturation-excess runoff model. *Water*, **11**(7), 1427. https://doi.org/10.3390/w11071427

Stringfield, V. (1966). *Artesian water in Tertiary limestone in the southeastern states* (No. 517-519). US Government Printing Office.

U.S. Fish & Wildlife Service (2018). National Wetlands Inventory. U.S. Fish & Wildlife Service. https://data.nal.usda.gov/dataset/national-wetlands-inventory. Accessed 2023-10-18.

Valayamkunnath, P., Barlage, M., Chen, F., Gochis, D., & Franz, K. (2020). Mapping of 30-meter resolution tile-drained croplands using a geospatial modeling approach. *Scientific Data*, **7**(1), 257. https://doi.org/10.1038/s41597-020-00596-x

White, E., Easton, Z., Fuka, D., Collick, A., Adgo, E., McCartney, M., *et al.* (2011). Development and application of a physically based landscape water balance in the SWAT model. *Hydrological Processes*, **25**, 915– 925. https://doi.org/10.1002/hyp.7876

White, M., Arnold, J., Bieger, K., Allen, P., Gao, J., Čerkasova, N., *et al.* (2022). Development of a field scale SWAT+ Modeling Framework for the contiguous U.S. *Journal of the American Water Resources Association*, **58**(6), 1545-1560. https://doi.org/10.1111/1752-1688.13056

Winter, T. (1999). Relation of streams, lakes, and wetlands to groundwater flow systems. *Hydrogeology Journal*, **7**, 28-45. https://doi.org/10.1007/s100400050178

Wu, K., & Xu, Y. (2007). Evaluation of the applicability of the SWAT model for coastal watersheds in southeastern Louisiana1. *Journal of the American Water Resources Association*, **42**(5), 1247–1260. https://doi.org/10.1111/j.1752-1688.2006.tb05298.x

Yan, L., & Roy, D. (2016). Conterminous United States crop field size quantification from multi-temporal Landsat Data. *Remote Sensing of Environment*, **172**, 67-86 https://doi.org/10.1016/j.rse.2015.10.034

Yimer, E., Bailey, R., Piepers, L., Nossent, J., & Van Griensven, A. (2023). Improved Representation of Groundwater–Surface Water Interactions Using SWAT+ gwflow and Modifications to the gwflow Module. *Water*, **15**(18), 3249. https://doi.org/10.3390/w15183249